DOE/ET/03425-21

BALANCE OF THE TROPOSPHERIC OZONE AND ITS RELATION TO STRATOSPHERIC INTRUSIONS INDICATED BY COSMOGENIC RADIONUCLIDES

Technical Progress Report

for Period November 1, 1980 - June 30, 1981

R. Reiter, H.-J. Kanter, R. Sladkovic, H. Jäger, and K.H. Munzert

Fraunhofer Institut
für Atmosphärische Umweltforschung
Kreuzeckbahnstrasse 19
D-8100 Garmisch-Partenkirchen, FRG

June 1981

Prepared for

THE U.S. DEPARTMENT OF ENERGY
AGREEMENT NO. DE-AC02-76-EV03425

DISCLAIMER

DOE/ET/03425-21

BALANCE OF THE TROPOSPHERIC OZONE AND ITS RELATION TO STRATOSPHERIC INTRUSIONS INDICATED BY COSMOGENIC RADIONUCLIDES

Technical Progress Report

for Period November 1, 1980 - June 30, 1981

R. Reiter, H.-J. Kanter, R. Sladkovic, H. Jäger, and K.H. Munzert

Fraunhofer Institut
für Atmosphärische Umweltforschung
Kreuzeckbahnstrasse 19
D-8100 Garmisch-Partenkirchen, FRG

June 1981

Prepared for

THE U.S. DEPARTMENT OF ENERGY
AGREEMENT NO. DE-AC02-76-EV03425

EAB

N O T I C E

Abstract

The balance of the tropospheric ozone is studied with regard to sources and sinks. The influx of stratospheric ozone through stratospheric intrusions and photochemical production under pure air conditions is discussed.

The 4-year measuring series (1977-1980) of the ozone concentration measured at 3 different levels (3000, 1800, 740 m ASL) are evaluated, the influence of meteorological parameters is examined. The time variation of the ozone layer between 1000 and 3000 m ASL is investigated as a function of different ozone sources.

First results show that stratospheric ozone arriving at the troposphere penetrates only in a few rare cases to the ground layer below 1500 m ASL. Most of the time, the variation of ozone concentration in this layer is determined by photochemical processes which are, in turn, controlled by meteorological parameters. The upper boundary of the photochemically active layer is found at about 500 m above ground.

The mean frequency distribution of stratospheric intrusions is shown to be independent of the season.

The possibilities of operating and calibrating the New Zealand filter photospectrometer are discussed.

Variability of the concentration of stratospheric aerosol and its optical properties after the volcanic eruptions in the year 1980 are discussed on the basis of lidar backscattering measurements.

1. GENERAL REMARKS

1.1 Scope of Work, Expenditure of Time and Funds

The works under contract with the U.S. Department of Energy have been performed pursuant to the provisions in Modification A004.
The general objectives were maintained. Expenditures for personnel and supplies/materials correspond to the cost estimate in our proposal of 10 July 1980.

1.2 Essential Characteristics

Activities during the reporting period can be grouped as follows:

I. Recording of ozone concentration at 3 different levels (3 km, 1.8 km, and 0.7 km ASL);

II. Aerosol sampling at station Zugspitze, chemical separation of cosmogenic radionuclides Be7, P32, P33, γ and ß-spectrometrical determination, respectively, of the nuclide concentrations;

III. Telemetrical measurements of the ozone profile between 1000 and 3000 m ASL by a cable car-borne ozone sonde;

IV. Study of the tropospheric transport mechanisms on two long-term periods from the year 1974 using the isentropic trajectory analysis of all available radiosonde data;

V. Classification of ozone sources in the lower troposphere based on data collected in the years 1977-80 as per I;

VI. Determination of the variation of the fine structure of the ozone profile in the lower stratosphere after solar events by means of daily balloon ascents up to 35 km altitude;

VII. Remote sensing of the stratospheric aerosol layer.

Items I and III serve to establish the ozone balance in the lower troposphere. By means of tracers obtained from II, stratospheric intrusions can be identified and their effects on the tropospheric ozone balance studied in connection with data obtained from I and III.

Item V provides first insights into the tropospheric ozone balance through assessment of possible ozone sources.

Point IV permits description of the tropospheric transport mechanisms. In conjunction with II, the interaction between stratospheric-tropospheric exchange and tropospheric transport can be described from the climatological point of view.

Through VII, light is thrown on the effect of solar events on the ozone profile in the lower stratosphere. The dynamic transport processes which can be read therefrom enhance the understanding of the stratospheric-tropospheric exchange.

By means of observations as per VII (e.g. volcanic eruptions) a possible anthropogenic contamination of the stratosphere can be assessed in relation to natural events.

2. ROUTINE WORK

2.1 Measurements of the Tropospheric Ozone

Measurements of tropospheric ozone at the stations Zugspitze (3 km), Wank (1.8 km), and Garmisch (7.4 km ASL) have been continued without interruption in the reporting period. Moreover, an ozone balloon sonde of type ECC 3-A could be modified such as to enable detection of the ozone profile from 1000 - 3000 m ASL. The cable car to the peak of the Zugspitze serves as sonde carrier. The ozone values, along with data of temperature, humidity, and air conductivity are telemetered to the base-line station at the Institute.

2.2 Aerosol Sampling

Aerosol sampling at the Zugspitze for obtaining tracers Be7, P32, and P33 was continued without problems. Difficulties arose in the spectrometrical measurements of nuclides Be7 and P33. Through fresh fallout after the Chinese nuclear test of 16.10.1980 it came, with the detector systems used so far - to a superposition of the peaks to be measured by fallout peaks. To overcome these difficulties we used from that time for measuring the Be7, a Ge-Li detector (high resolution but poor counting statistics) instead of the previously used NaJ - detector (poor resolution at very good counting statistics).

The difficulties could not be eliminated in the case of P33 measurements since, with the liquid scintillation counting used, no better resolution can be achieved and a foregoing chemical separation of the interfering nuclides proved impracticable. Thus, the P33 values from the period in question must be rejected.

2.3 Measurement of Total Ozone with a New Zealand Filter Photospectrometer

The studies concerning usability of the filter photospectrometer were continued. A summary of previous results and a critical weighting of the difficulties met is given in chapter 4.2.

2.4 Balloon Soundings of the Ozone Profile up to 35 km Altitude

Altogether, 8 series of ozone sonde ascents were carried out during the reporting period. Three of those fell within the last quarter of 1980 and five in the year 1981. In time sequence flown were in each case 17, 8, 4, 8, 5, 12, 4, and 8 balloon sondes, respectively. The series of ascents were initiated after announcements (in URSIGRAM) of violent solar events. In the recent past (since April 1981) the flights can be started essentially more acute through observation of the density of thermal neutrons by an institute-owned neutron monitor. One of the afore mentioned series was flown after announcement of a sudden warming over northern Europe. The stratospheric warming could also be observed in our latitude.

2.5 Monitoring of Stratospheric Aerosol

In the reporting period the effects of the eruption of volcano Mt. St. Helens on the stratospheric aerosol layer could be documented by routine lidar observations (see also chapter 4.3).

3. CURRENT EVALUATIONS

On the basis of round 10-year measuring series of tracers Be7, P32, and in connection with ozone measurements which were started later (1978), the evaluations described below are being processed. Jointly they shall serve to establish a climatology of the stratospheric-tropospheric exchange.

3.1. Determination of Transport Processes in the Stratosphere

For selected periods isentropic trajectories are used to determine the routes of transport along which stratospheric air after injection is brought to the measuring site.

The periods were selected according to possible seasonal effects. To cover this aspect 3 long-term periods have been considered:

Period A: 20.02.1974 - 25.05.1974 (94 days)

Period B: 20.07.1974 - 20.09.1974 (62 days)

Period C: 01.10.1974 - 08.10.1974 (8 days).

From a comparison with the tropospheric flow conditions during periods without intrusions information is expected about the coupling between stratospheric-tropospheric exchange and large-scale transport between tropopause and boundary layer. Seasonal variations can be explained by the above material.

In order to ensure a consistent scientific processing a meteorologist was temporarily engaged alone for the task of concluding this very time-consuming work in the near future. The results will be presented in Annual Report Part IX.

3.2. Calculation of the Residence Time of Air in the Lower Stratosphere

By means of activity ratio P32/Be7 determined for individual intrusions, the mean residence time of air in the lower stratosphere is estimated. Seasonal differences will be clarified. The principles of processing have been agreed with Prof. Dr. Elmar R. Reiter, Colorado State University. The theory used in the calculation correspeonds to that described earlier by E. R. Reiter (1975)[+]).

3.3. Correlation Between Be7 and Ozone

It has been attempted to deduce from the correlation between ozone (measured at the Zugspitze) and Be7 the influence of stratospheric intrusions on the ozone budget. First results proved unsatisfactory. In a new attempt the ozone values will prior to the correlation calculation be corrected such that the superposed annual variation is suppressed.

3.4. Correlation Between Be7 and Pb 210

Since January 1975, Pb 210 is determined on weekly samples of aerosol collected at the Zugspitze (see 2.2). This is done γ-spectrometrically by a hyper pure germanium detector.
In a first evaluation these measured values will be compared with time-coincident Be7 weekly mean values in a correlation calculation.

[+]) Reiter, E.R., Carnuth, W., Kanter, H.J., Pötzl, K.,Reiter R., and Sladkovic, R.: Measurement of stratospheric residence times. Arch.Met.Geophys.Biokl., 24, Ser.A, 41-51 (1975)

4. RESULTS

4.1. Ozone Sources in the Lower Troposphere

On the basis of ozone recordings from the stations Zugspitze (3 km), Wank (1800 m), and Garmisch (740 m) of the years 1977 - 1980 we show in the following systematic differences in the behavior of ozone in the layer from the valley floor up to maximum 1000 m above the valley and the overlying region.

A first evaluation of ozone profiles obtained by the cable car telemetry system gives information about the ozone stratification in the lower troposphere. Ozone sources observed therefrom are discussed.

4.1.1. Mean diurnal variations per station and per month for the period 1977 - 1980

Fig. 1 shows the mean diurnal variation per month and station from the total 4-year measuring period for all recording days. The capital letters in the fields denote the months (January, February, etc., till December). It is surprising that the amplitude of the daily variation, if any, (in January and December it is e.g. absent) is extremely low at both mountain stations and that the absolute monthly mean values at the mountain stations Zugspitze and Wank are practically in agreement with each other, aside from slight irregular deviations. Conspicuous is, however, that the O_3 daily variation is most pronounced at the valley station and is obviously dependent on the season. In winter the amplitude is very low.

In the months of January, February, November and December it is remarkable that before the afternoon peak in Garmisch (valley) a week, yet well defined, minimum is observed between 7.00 and 11.00 hours. Interestingly, these are exactly the same

periods and exactly the same months in which CO_2 and SO_2 in the valley show maximum values. This means, that during the time of the passage of the pollution plume from Garmisch-Partenkirchen past our Institute due to the valley wind, the ozone concentration is temporarily reduced by other reactive gases such as mainly NO, and possibly SO_2.

Furthermore it is remarkable that the ozone maximum occurs in the early afternoon. Between April and July, the ozone concentrations exceed for a short time the values of at least one of the mountain stations. For the the total period we selected therefore in another diagram only such days in which relative sunshine duraration was >80% without precipitation. Results from the the valley station and Zugspitze are shown in Figs. 2a and 2b. If we compare these diagrams with Fig. 1, it is obvious at once that the afternoon peak values at the valley station (740 m) are essentially higher than on average days while conversely no remarkable changes are found at the station Zugspitze.

The data in Fig. 1 und 2 show also the annual variation of O_3 at the mountain stations. The annual variations at all three stations can be seen from Fig. 3. The lowest values, mainly in the valley, occur in the cold season and the highest values in the warm season. On the average, the O_3 concentration is lower in the valley (G) than at the mountain stations Z and W whose O_3 data are in reasonable agreement. The concentrations at Z and W are in conformity with the equinoctial periods.

Comparing Fig. 2a and Fig. 1 permits the conclusion that in the surface layer at intense solar radiation and under pure air conditions there must be an additional ozone source for all other relevant recordings in the valley show that under

conditions as assumed in Fig. 2a neither local or regional pollution could have existed, nor transport from polluted areas north of the Alps was involved.

In Fig. 4, the data have finally been classified according to spring and summer until early fall, inclusively. On cloudy days (Fig. 4 b,d) appears indeed a well defined and significant afternoon maximum of the ozone concentration. However, on exclusively sunny days (Fig. 4 a,c) essentially higher peak values are reached in the afternoon exceeding in all cases the values simultaneously measured at the mountain stations. Hence it follows that we have here primarily an influence of irradiation (Fig. 4 a,c versus Fig. 4 b,d) which is however additionally superposed by an effect of temperature (maximum between 14 - 16^{o}C).

In other words, we find in the case of Fig. 4 quite obviously in the valley at low altitude a photochemical source of ozone which is not affected or caused by local or regional air pollution. It also follows clearly from Fig. 4 that no vertical transport of stratospheric air down to lower altitudes is involved because during intense sunshine the ozone gradient between Zugspitze and valley is reversed.

Now, there arises first of all the question as to the thickness of the layer in the lowest troposphere in which photochemical production of ozone takes places under pure air conditions.

4.1.2. Ozone profiles between valley and Zugspitze

In early 1980, the ozone radiosonde was installed in our Zugspitze cable car telemetry system. These profile measurements were made only under suitable weather conditions, i.e., by no means during precipitation. Nevertheless about 1000

vertical profiles have been taken on 65 measurement days until March 1981. A statistical evaluation of this extensive and complex material cannot be presented at this time.

However, it will be shown for two typical days that we have no doubt two distinctly different ozone sources in the troposphere. On Figs. 5 and 6 are plotted respectively in time sequence (time above the O_3 profiles in 5a, 6a) in line a the ozone profiles, in line b the temperature profiles, and in line c the profiles of the positive conductivity of the air (which can be regarded as a measure of the aerosol particle concentration). The scales for ozone concentration and temperature are given respectively in the left, the electrical conductivity is indicated in relative units increasing from 0 to the right.

In one of the bottom lines (d) the variation of the ozone concentration from measuring run to measuring run are plotted for given height levels as continuous curves. In this manner we obtain the time variation between 1.1 and 3.0 km at height intervals of 400 m.

First we look at Fig. 5. All over the day, the ozone concentration (line a) increases with height. In the forenoon we observe at first a relatively steep increace between 2.0 and 2.5 km. In the afternoon, however, there is a striking increase in the ozone concentration immediately at the Zugspitze (3.0 km) with a sharp lower boundary at 2.7 km. From 1400 h we observe a marked subsidence visible through a steepening of the temperature gradient (line b): From noon, we find practically isothermal layers at altitudes from 2.8 to 3.0 km. The additional amount of ozone, obviously of stratospheric origin, does not penetrate to lower altitudes. From line d it is clearly evident that in field 3.0 (km height) a well pronounced rise of the ozone concentration occurs throughout

the day which does, however, no longer exist at 2.6 km altitude. The weak increases in ozone concentration observed at lower levels are likely to be due to local photochemical production and are not influenced by the ozone intrusion from the stratosphere which prevailed down to 2.7 km altitude. Interesting is the comparison with the time behavior of the electrical conductivity (line c). We note good agreement with the behavior of the ozone concentration: In those atmospheric layers where we find distinctly elevated ozone concentrations, the electrical conductivity is also markedly increased. This concerns in the forenoon the layer rising from about 2.0 to 2.5 km (i.e., above this stated limit) and especially the increased conductivity values in the afternoon above 2.7 km, meaning thus the region in which the stratospheric intrusion prevailed.

Fig. 5 shows representatively of many analogous cases that there is no doubt a stratospheric ozone influx to the middle or lower troposphere but a breakdown of stratospheric ozone to levels lower than 1.5 km ASL is extremely rare.

On Fig.6 we view the reverse case. At an altitude of about 2 km ASL the ozone concentration (line a) remains constant as can also be seen from the time trends in fields 3.0, 2.6, and 2.2 in line d. Only at 1.8 km altitude and mainly below we find in the course of the day a marked increase in the ozone concentration which is clearly evident from line a, and also from the fields in line b between 1.8 and 1.1 km altitude. In line a it is moreover very clear pronounced (in contrast to Fig. 5) how the nocturnal ozone deficit (in the morning the ozone concentration increases steeply with height) is gradually replenished until the afternoon. Then, the O_3 concentration is higher in the valley and

decreases to the Zugspitze level. The confinement of the photochemical ozone layer towards higher levels is favored in part by a temperature inversion (line b) which persisted from the morning to late noon. But even under good exchange conditions and in the absence of the temperature inversion in the afternoon is does not come to a homogeneous mixing between the valley and the level of the Zugspitze. The electrical conductivity (c) shows no marked profile changes but reveals nevertheless a kink in the height of the temperature inversion, mainly at noon and in the early afternoon (higher conductivities above). Now, Fig. 6 shows us - in contrast to Fig. 5 - the photochemical ozone source in the lower troposphere and permits us to assess simultaneously that the thickness of the layer may extend from the ground (0.7 km) to about 1.5 or 1.8 km ASL. Our recordings from station Wank show, however, that at a level of 1.8 km a photochemical production process can be neglected in the majority of cases. Hence we can say, that photochemical ozone production takes place in a layer of maximum 1.0 km thickness from the ground. On the average - as our Zugspitze cable car recordings indicate - the layer with a photochemical source may have a thickness of about 500 m.

Thus it is also clarified that natural, relatively high ozone concentrations are obviously produced in pure air regions of the biosphere where mainly in the warm and radiation-intensive season values of 80 ppb, in rare cases nearly 100 ppb can be measured.

4.2. Measurement of the Total Ozone with a New Zealand Filter Photospectrometer

As is known from previous reports, a New Zealand filter photospectrometer is used in Garmisch-Partenkirchen for measuring the total ozone. The data obtained are currently checked by intercomparisons with the neighboring Dobson stations Hohenpeissenberg and Arosa.

4.2.1. Measuring technique

The filter photometer functions in 6 wavelength ranges by which the X_{AD}, X_{AC}, and X_{CD} values are calculated through ratio and subtraction of the individual channels.

The 305.5 nm filter which was removed in January 1980 could be replaced and calibrated only in October 1980 due to problems in manufacturing. Because of the low position of the sun, calibration could be repeated not before March 1981. In the observational period of 5 months appeared again a drift of the filter so that in April 1981 the 3rd defective 305.5 nm filter had to be removed. The X_{AD} and X_{AC} values during the winter period are useless despite all corrections. Thus, it was not yet possible to produce for this filter photospectrometer the needed 305.5 nm filter with 1.5 nm band width at half peak transmittance of sufficient stability. Besides, only one company at all is willing to construct such a filter. That's why only values in the CD range are available since 1978.

Calibrations for the CD pairs yielded very good results, the calibration constants I_{CD} (logarithm of the ratio of extraterrestrial intensities) shifted, however, from 0.57 in February 1980 to 0.62 in April 1981 and the constant $\Delta\alpha_{CD}$ (difference of the ozone absorption coefficient) from 0.440 to 0.448 in the same period. Adaption of $\Delta\alpha$ proved necessary since a systematic change of the calculated total ozone was shown as a function of the relative air mass indicating an

error in the constants. The instrument, with this uncertainty in $\Delta\alpha$, is therefore only a relative instrument as for each calibration for determining $\Delta\alpha$ the total ozone content must be known in an other way. Control of the acquired values is complicated by the fact that the instrument due to filter removal delivers only one value (X_{CD}) instead of the three values originally designed by the manufactuer and did not get beyond the laboratory status of testing. A steady comparison with the nearby Dobson stations is thus unavoidable. The single measurements of the filter photospectrometer show fairly constant a standard deviation of 5 DU at 5 - 30 measurements per day.

4.2.2. Comparison with Dobson values

Since March 1978, the CD filter values from Garmisch-Partenkirchen were by 6.8 DU too high as compared to the Dobson values from Arosa at a standard deviation of 6.1 DU.

Linear regression over 11 identical days each provided in March 1980

$$X_{CD\ GAPA} = 1.03 \cdot X_{AD\ AROSA} - 7\ DU; \qquad r^2 = 0.95$$

and in September 1980

$$X_{CD\ GAPA} = 1.04 \quad X_{AD\ AROSA} - 6\ DU; \qquad r^2 = 0.97$$

In March 1981, where unfortunately no comparative values from Hohenpeissenberg are available, a calculation over 9 days yielded due to the high variability of the total ozone

$$X_{CD\ GAPA} = 0.90 \quad X_{AD\ AROSA} + 41\ DU \qquad r^2 = 0.80$$

A better substantiation of the inherently good CD values fails because of the uselessness of the AD and AC values. An improvement of this situation through a reliable 305.5 nm filter is promised by the manufacturer.

4.3. Lidar Monitoring of the Stratospheric Aerosol Layer

The year 1980 was distinguished by a number of volcanic events. Mount St. Helens, Washington, USA, erupted violently on 18 May with subsequent eruptions in June, July, August, and October. All these eruptions were reported to penetrate into the stratosphere, the first one reaching an altitude of 23 km. On 17 August the volcano Hekla on Iceland added to the deposition of volcanic debris in the stratosphere. These were the first major events of volcanism since the eruption of the volcano Fuego, Guatemala, in October 1974. They terminated the period of background aerosol prevailing in the stratosphere since the end of 1976, after the decay of the volcanic aerosols injected by the Fuego eruption in 1974. The 1980 volcanism transported large amounts of gaseous and solid material into the stratosphere, leading to a substantial enhancement of the stratospheric aerosol layer.

The St. Helens eruption cloud was transported to the German Ocean via the east coast of the North American continent, the North Atlantic, and the south coast of Greenland. The arrival of the cloud over mid-Europe was determined by in-situ sampling, lidar observations and trajectory calculations.

Since the first eruption of St. Helens on 18 May until the end of 1980, 37 stratospheric aerosol profiles have been measured. The first lidar sighting of the St. Helens cloud most probably was the peak found at 11 to 12 km on 25 May evening. Figure 7 shows 16 stratospheric aerosol profiles, commencing on 25 May; the last one dates from 14 July. All measurements had to be performed during night time to eliminate diffuse sky light radiation. For comparison the 1979 average profile is plotted as the first profile. This is the mean of 21 soundings, with R_{max} = 1.07 at 18 km and R_{min} = 1.03 at 25 km.

The profiles 25 May to 9 June show this 1979 background profile above 15 km approximately. The aerosol peak of 30 May for the first time appears separated from the tropopause. On 9 June a dense cirrus layer almost obscured the aerosol peak. On 12 June two aerosol layers appear. Thereafter, the stratospheric aerosol is multi-layered. The top altitude was reached on 30 June with a sharp upper layer boundary at 24 km, 43 days after the first eruption. The highest scattering ratios were measured on 5 July with R=2.5 at 15.3 km and R=3.4 at 22.5 km and on 14 July with R=4.8 at 21.3 km. A sharp decrease of the backscattering signal after 14 July was followed by a steady decline of the signal intensity from the end of July until the end of 1980 (see Fig. 9).

The lidar profiles presented in Fig. 7 indicate that with increasing time after the first St. Helens eruption the aerosol layers are seen at increasing height levels. That can be observed until 22 June with an upper boundary of the volcanic aerosol at 17 km. On 30 June an aerosol layer appears at 23.5 km. During the weeks following that date the altitude of the uppermost aerosol layer decreases. This observation is in good accordance with the circulation profile, which has been derived from the Munich radiosonde for the period May to August 1980: below 19.5 km the transport direction is from west, above this level from the east (Fig. 8). Assuming little vertical transport and mixing of the aerosol layers which have been formed by diverse air motions immediately after the first St. Helens eruption, the highest aerosol layer at a time can be attributed to the first eruption, and up to 19.5 km the arrival of layers at increasing height levels must be delayed by the reduced transport speed. Above 19.5 km the transport speed increases again (although the direction has changed by 180 degrees) so that the part of the eruption cloud which had reached the highest level in the stratosphere could be observed at an earlier date than layers at 22 or 21 km. The transport routes

differ by about 50%, the route from the west being the shorter one.

The arrival dates and the estimated transport distances yield transport speeds which are also presented in Fig. 8. The lidar determined transport speeds correspond well with the general circulation deduced from the Munich radiosonde.

Figure 9 shows a comparison of the maximum optical mixing ratio (maximum scattering ratio - 1) with the height integrated backscattering coefficient (integrated from tropopause level + 1 km to approximately 26 km, the upper limit of the aerosol layer). The mixing ratio rises by a factor of 26 above the January to May value, whereas the integral backscattering increases by a factor of 4.5. This difference is explained by the high values of the mixing ratio which have been measured above 20 km (Fig. 7) and which are a result of the reduced molecular scattering at higher altitudes. The absolute volcanic aerosol load of the stratosphere is much higher at lower height levels. A sharp decrease of the backscattering signal after 14 July was followed by a steady decline of the signal intensity from the end of July until the end of 1980. After end of July the mixing ratio declined with a half-life of 5 months, the integrated backscattering with 7 months. The faster decrease of the mixing ratio can be explained by a more rapid sedimentation of aerosol particles at higher altitudes. This has been investigated in more detail in Fig. 10, where the integrated backscattering coefficient again is presented for the 1980 period, but the lower integration limit has been varied in steps from 10 to 21 km. All courves show background conditions until beginning of June, the integrals 10-26 and 12-26 are slowly rising (probably due to a distribution of volcanic debris at low stratospheric levels originating from the Sierra Negra eruption, Galapagos, November 1979). Until the middle of July the backscattering

intensity increased, the magnitude of the increase depends on the lower limit of the integral: From a factor 3 for the 10-26 km integral to a factor 18 for the 21-28 km integral. This pronounced relative enhancement of backscattering at high altitudes corresponds with the high scattering ratios above 20 km (Fig. 7). On the other hand the absolute values of the integrated backscattering show that most of the volcanic aerosol was deposited between 10 and 15 km altitude. After end of July the 10-26 and 12-26 km layers show relatively long decay rates which can be explained by aerosol supply at low altitudes by the St. Helens eruptions during June to August and the Hekla eruption in August. The relatively fast decay at high altitudes points to a transport of relatively heavy particles by the first St. Helens eruption up to great heights with subsequent rapid sedimentation; at the end of 1980 the 21-26 km integral almost was at the pre-Helens level. The short decay times of the 10-26 and 12-26 km integrals towards the end of 1980 can be explained by the short observation time of a still inhomogeneously distributed St. Helens aerosol.

The curves of Fig. 11 are the result of the application of stratospheric aerosol models to the integral backscattering coefficient shown in Fig. 3. The optical depth τ is defined as

$$\tau = \int_{h_1}^{h_2} \alpha_p \, dh$$

and the transmission q is defined as

$$q = e^{-\tau}.$$

α_p is the particulate extinction coefficient, h_1 the tropopause level + 1 km and h_2 is the upper boundary of the aerosol layer. The particulate extinction coefficient can be derived from the lidar measured particulate backscattering coeffi-

cient β_p :

$$\alpha_p = \beta_p \cdot \frac{4\pi}{P(\pi)}$$

$P(\pi)/4\pi$ is the backscattering phase function, which is determined by aerosol properties like size distribution, composition, and refractive index. Literature values for $P(\pi)/4\pi$ range from .013 to .049. For the evaluation of the optical depth $P(\pi)/4\pi$ = .015 has been adopted, which is the mean of three aerosol models (Haze H, lognormal, Zold), with a refractive index m = 1.42 + 0i and a composition of 75% H_2SO_4 + 25% H_2O.

The enhancement of the stratospheric aerosol layer yielded a maximum transmission reduction of 1.5% at the wavelength of the lidar system. At the end of 1980 the transmission was still reduced by 0.3%.

4.4. Frequency of Stratospheric Intrusions

As a first step towards a climatology of the stratospheric-tropospheric exchange the 10-year measuring series has been analyzed for the frequency of stratospheric intrusions. The concept of the "stratospheric intrusion" has been determined by the following two definitions:

Criterion A: As stratospheric intrusion are counted month-by-month all Be7 peaks which exceed the monthly mean value of the Be7 concentration by at least 30%.

Criterion B: As stratospheric intrusion are counted all Be7 peaks which exceed the monthly mean value of the Be7 concentration by at least twice its standard deviation.

In the case of criterion B the meteorologically-induced scatter in the data should be considered through inclusion of the standard deviation of the individual values since this, as earlier reported, shows seasonal differences.

In the evaluation according to both criteria events of duration longer than one day have been counted only once.

In the table below, the results are presented as mean montly frequency of the occurrence of stratospheric intrusions.

CRIT	month	J	F	M	A	M	J	J	A	S	O	N	D
	No of ys.	11	11	11	10	10	10	11	11	11	11	12	12
A	mean frequ.	4.09	3.91	4.18	3.7	3.8	3.6	3.64	3.73	3.55	3.64	3.92	3.58
	stand.dev.	1.37	0.70	0.75	1.34	1.23	0.52	0.67	1.35	0.82	0.50	1.16	1.08
B	mean frequ.	3.09	3.09	3.18	3.20	3.1	2.8	2.45	3.27	2.63	2.72	3.25	2.67
	stand.dev.	1.30	0.94	1.25	1.13	1.52	0.92	0.69	1.10	1.12	0.90	1.22	0.65

Neither according to criterion A, nor according to criterion B, any significant seasonal differences, checked by variance analysis (F-test) according to R.A. Fischer, can be observed. Consequently, the frequency of the occurence of stratospheric intrusions is evenly distributed throughout the year.

FUTURE PLANS

1. Continuation of ozone recording at 3 different levels of the boundary layer (700 m, 1800 m, and 3000 m a.s.l.), measuring of the ozone profile between 1000 m and 3000 m ASL by means of a cable car-borne ozone sonde.

2. Continuation of aerosol sampling at the Zugspitze, analysis of cosmogenic radionuclides Be7, P32, P33 to identify stratospheric intrusions; study of the influx of stratospheric ozone after intrusions; assessment of their contribution to the tropospheric ozone balance; clarification of the conditions under which photochemical production takes place under pure air conditions.

3. Climatological evaluation of the 10-year measuring series of Be7 and P32; calculation of the mean residence time of tropospheric air in the lower stratosphere from the activity ratio P32/Be7; determination of the correlation between Be7 and ozone (measured at 3000 m ASL); distribution of stratospheric intrusions according to frequency and intensity.

4. Monitoring of the variation of the ozone profile in the lower stratosphere for selected periods of time by balloon-sondes, studies of a possible control of the ozone layer by solar events.

5. Lidar observation of the stratospheric aerosol layer, assessment of the life time of volcanically-related aerosol.

Dr.R. Reiter
Director

Garmisch-Partenkirchen

Legends of Figures

Fig.1 : Monthly-averaged daily variation of the ozone concentration measured at 3 different altitudes of the lower troposphere
total of all days 1977/80

Fig.2 : Monthly-averaged daily variation of the ozone concentration measured on days with rel. sunshine duration >80%

a) Station Garmisch 740 m a.s.l.

b) Station Zugspitze 3000 m a.s.l.

Fig.3 : Ozone monthly mean values for the years 1977-1980 for 3 different altitudes

Fig.4 : Dependence of the ozone concentration at different levels of the boundary layer on season and relative sunshine duration

Fig.5 : Time variation of the ozone profile in the lower troposphere (1000 - 3000 m a.s.l.), temperature and aerosol stratification during influx of stratospheric ozone after a stratospheric intrusion

Fig.6 : Time variation of the ozone profile in the lower troposphere through photochemical production in the ground layer

Fig.7 : Lidar observations (backscattering ratios) of the formation of aerosol layers in the stratosphere after the St. Helens eruptions. Measurements were performed late in the evening or very early in the morning (as indicated by double date). T denotes the Munich radiosonde tropopause

Fig.8 : Vertical profile of the atmospheric circulation derived from the Munich radiosonde compared with transport speeds observed by the IAU lidar

Fig.9 : Time variability of the maximum scattering coefficient -1 (optical mixing ratio) and the height integrated particulate backscattering coefficient (integrated from tropopause + 1 km to upper layer boundary at about 26 km)

Fig.10: Time variability of the height integrated particulate backscattering coefficient for different height intervals

Fig.11: Time variability optical depth and transmission

F I G U R E S 1 - 11

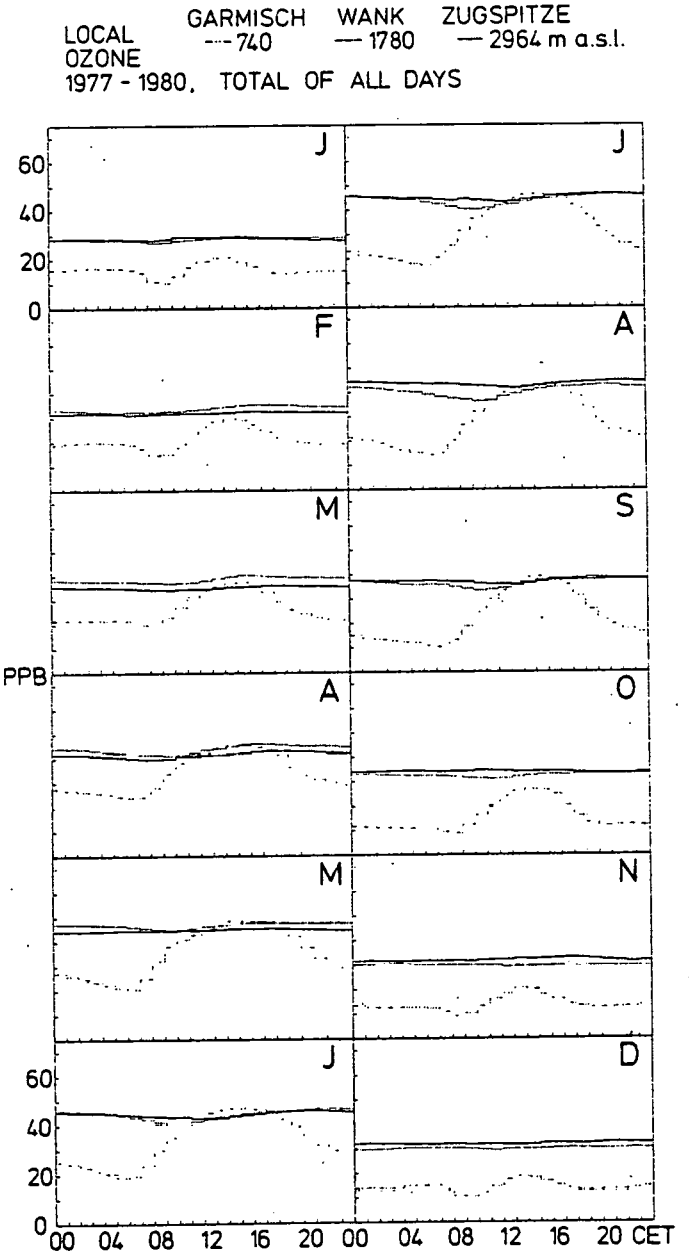
LOCAL OZONE
1977 - 1980, TOTAL OF ALL DAYS
GARMISCH --- 740
WANK — 1780
ZUGSPITZE — 2964 m a.s.l.
J
J
F
A
M
S
A
O
M
N
J
D
60
40
20
0
PPB
00 04 08 12 16 20 00 04 08 12 16 20 CET

Fig.1

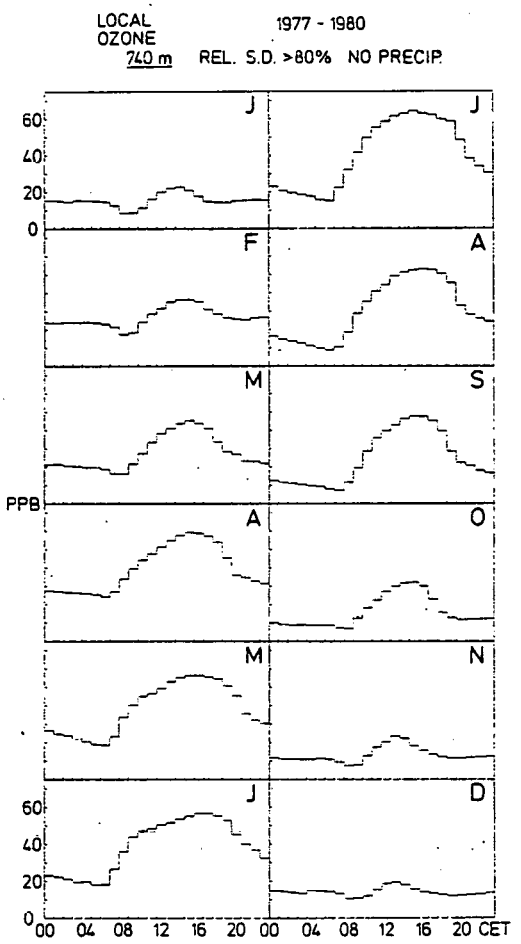
LOCAL
OZONE
740 m
1977 - 1980
REL. S.D. >80% NO PRECIP.
J
J
F
A
M
S
A
O
M
N
J
D
PPB
60
40
20
0
00 04 08 12 16 20 00 04 08 12 16 20 CET

a

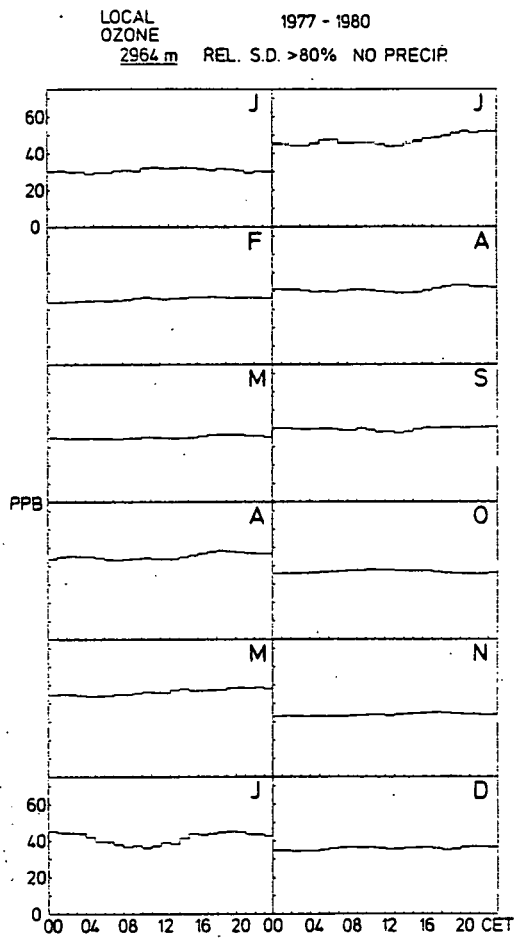
LOCAL
OZONE
2964 m
1977 - 1980
REL. S.D. >80% NO PRECIP.
J
J
F
A
M
S
A
O
M
N
J
D
PPB
60
40
20
0
00 04 08 12 16 20 00 04 08 12 16 20 CET

b

Fig.2

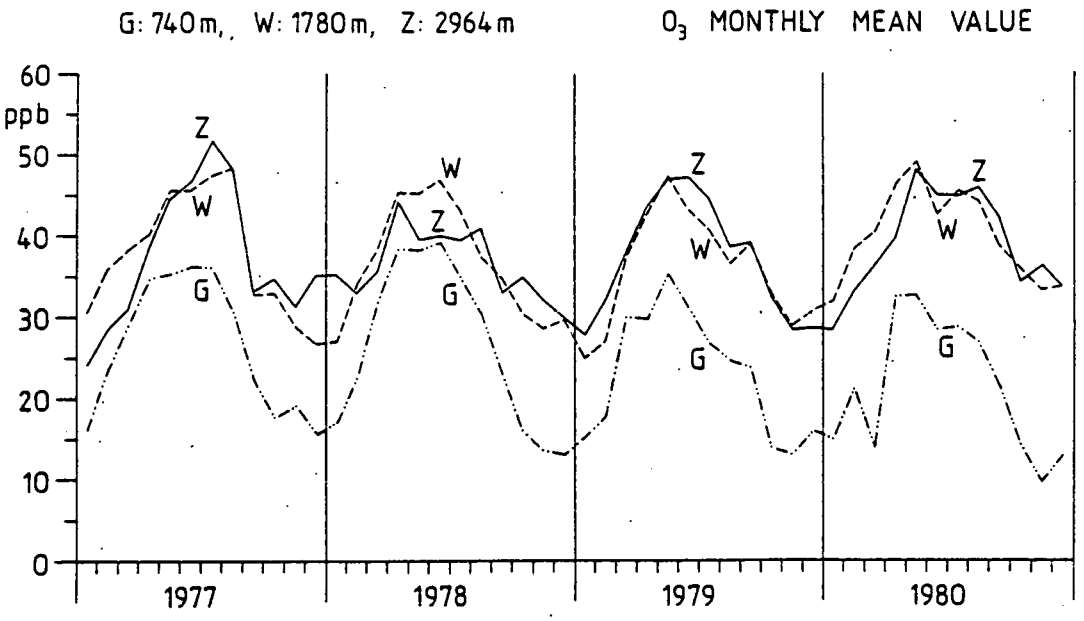
G: 740 m, W: 1780 m, Z: 2964 m
O_3 MONTHLY MEAN VALUE
ppb
60
50
40
30
20
10
0
Z
W
G
1977
1978
1979
1980

Fig.3

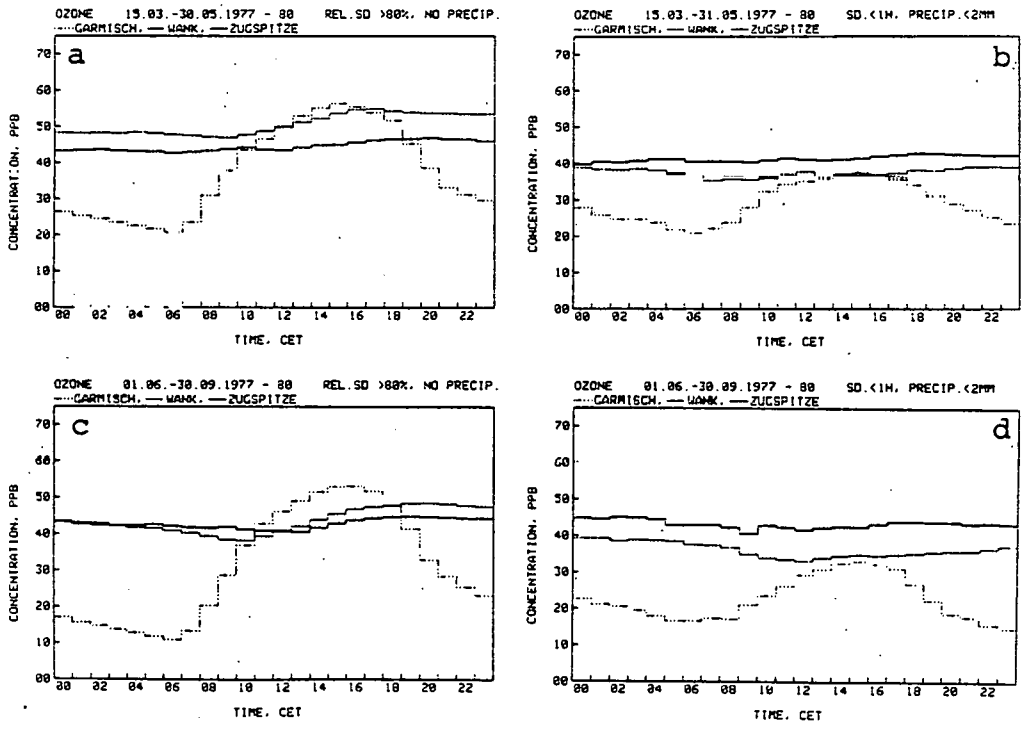
OZONE 15.03.-30.05.1977 - 80 REL.SD >80%, NO PRECIP.
GARMISCH. — WANK. — ZUGSPITZE
a
CONCENTRATION, PPB
TIME, CET
OZONE 15.03.-31.05.1977 - 80 SD.<1H, PRECIP.<2MM
GARMISCH. — WANK. — ZUGSPITZE
b
CONCENTRATION, PPB
TIME, CET
OZONE 01.06.-30.09.1977 - 80 REL.SD >80%, NO PRECIP.
GARMISCH. — WANK. — ZUGSPITZE
c
CONCENTRATION, PPB
TIME, CET
OZONE 01.06.-30.09.1977 - 80 SD.<1H, PRECIP.<2MM
GARMISCH. — WANK. — ZUGSPITZE
d
CONCENTRATION, PPB
TIME, CET

Fig.4

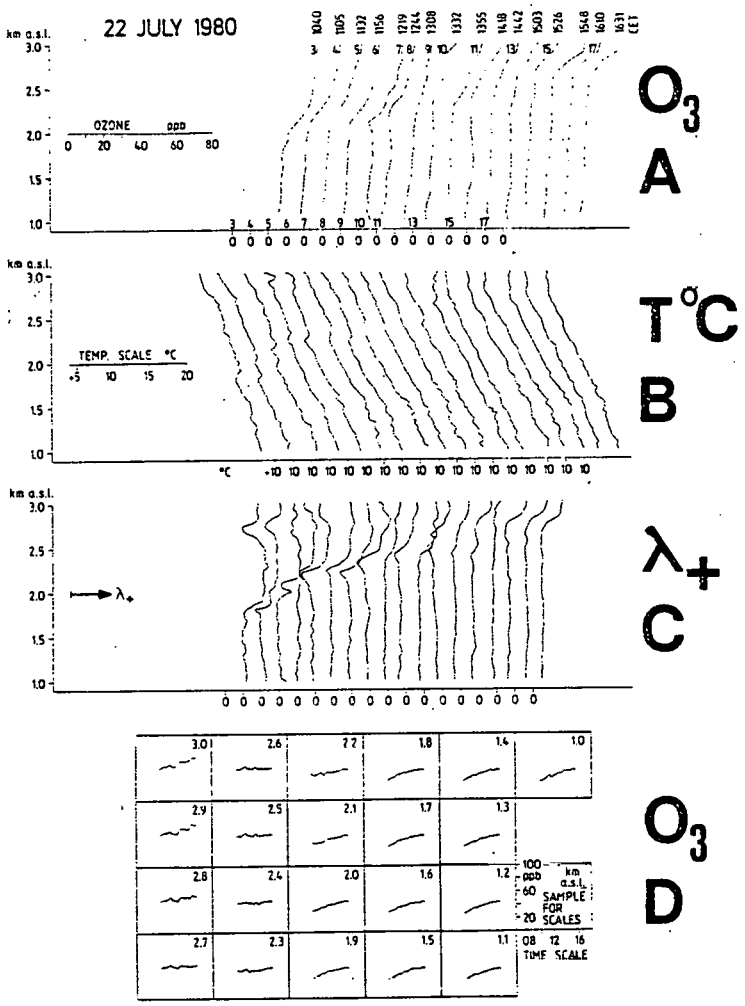
22 JULY 1980
km a.s.l.
OZONE ppb
0 20 40 60 80
O_3
A
TEMP. SCALE °C
+5 10 15 20
T°C
B
λ_+
C
O_3
D
100 ppb
60
20
km a.s.l.
SAMPLE FOR SCALES
08 12 16
TIME SCALE

Fig.5

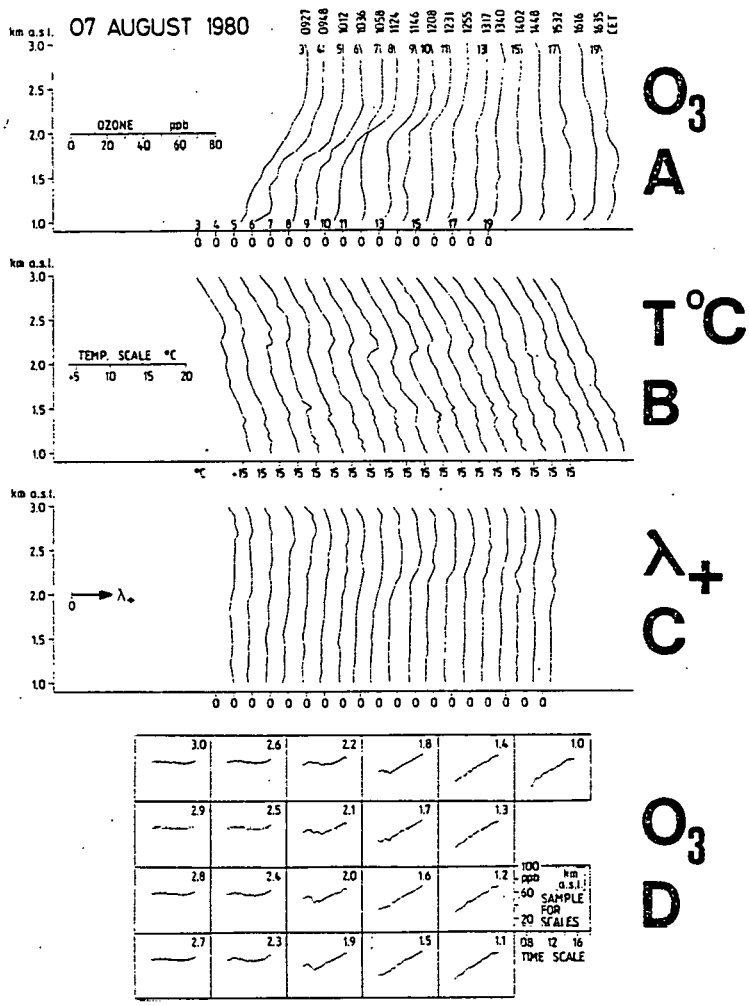
07 AUGUST 1980
km a.s.l.
OZONE ppb
0 20 40 60 80
TEMP. SCALE °C
+5 10 15 20
λ+
O3
A
T °C
B
λ+
C
O3
D
SAMPLE FOR SCALES
TIME SCALE
08 12 16

Fig.6

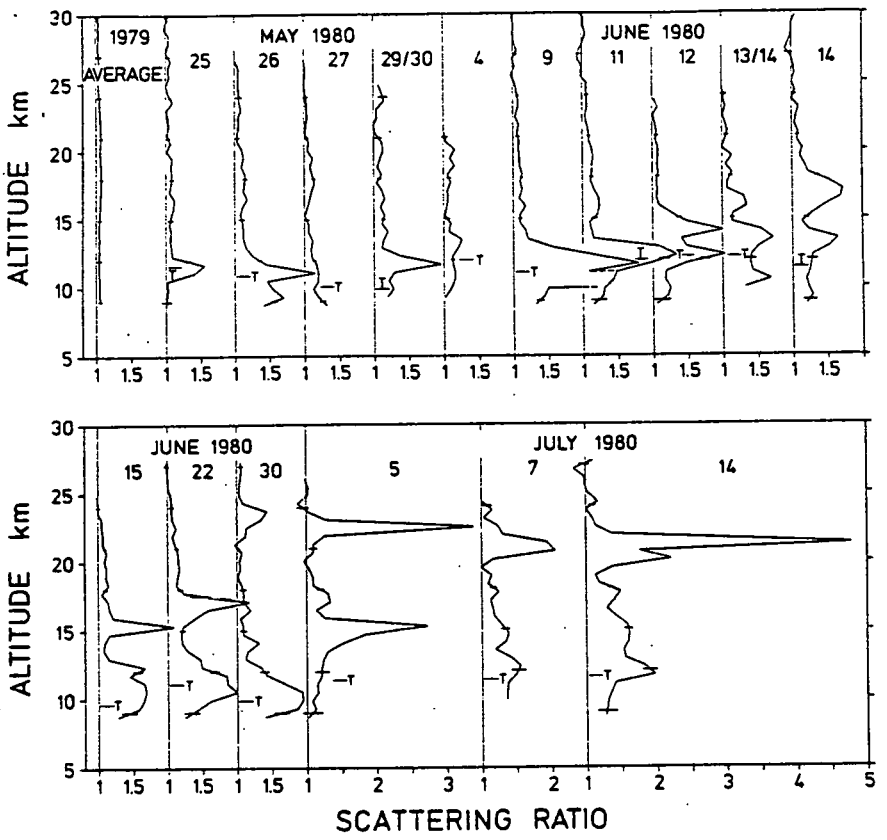
1979
AVERAGE
MAY 1980
25
26
27
29/30
4
JUNE 1980
9
11
12
13/14
14
JUNE 1980
15
22
30
JULY 1980
5
7
14
ALTITUDE km
SCATTERING RATIO

Fig.7

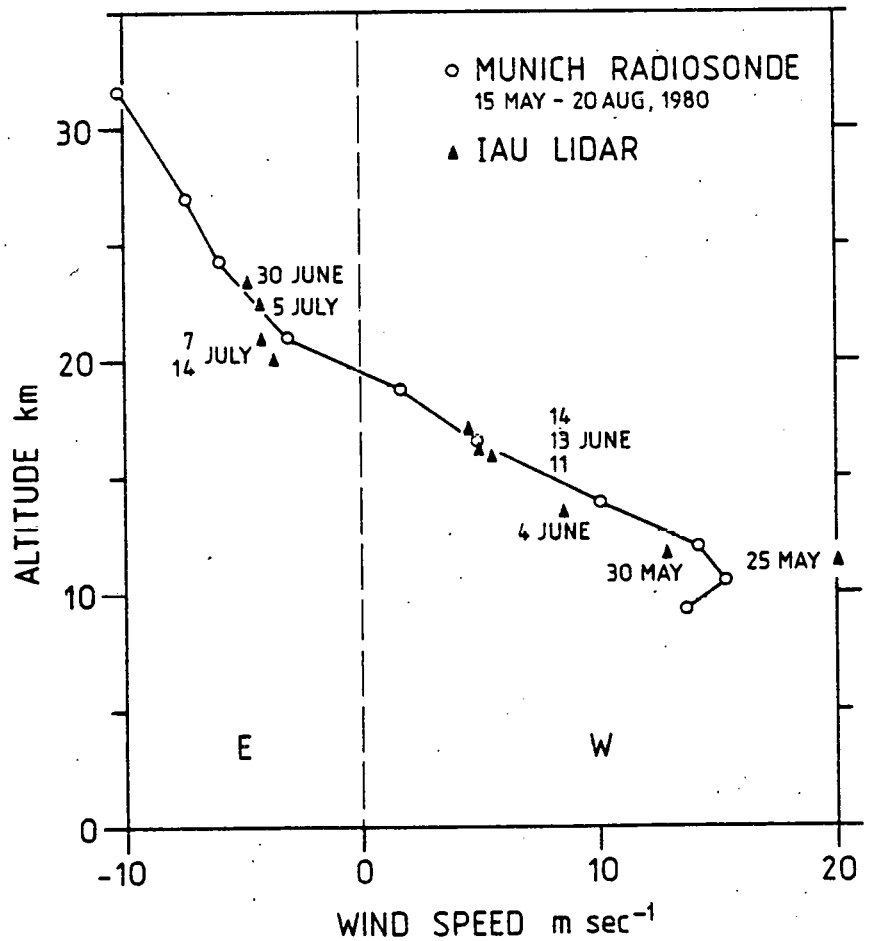
MUNICH RADIOSONDE
15 MAY - 20 AUG, 1980
IAU LIDAR
30 JUNE
5 JULY
7
14 JULY
14
13 JUNE
11
4 JUNE
30 MAY
25 MAY
E
W
ALTITUDE km
WIND SPEED m sec⁻¹

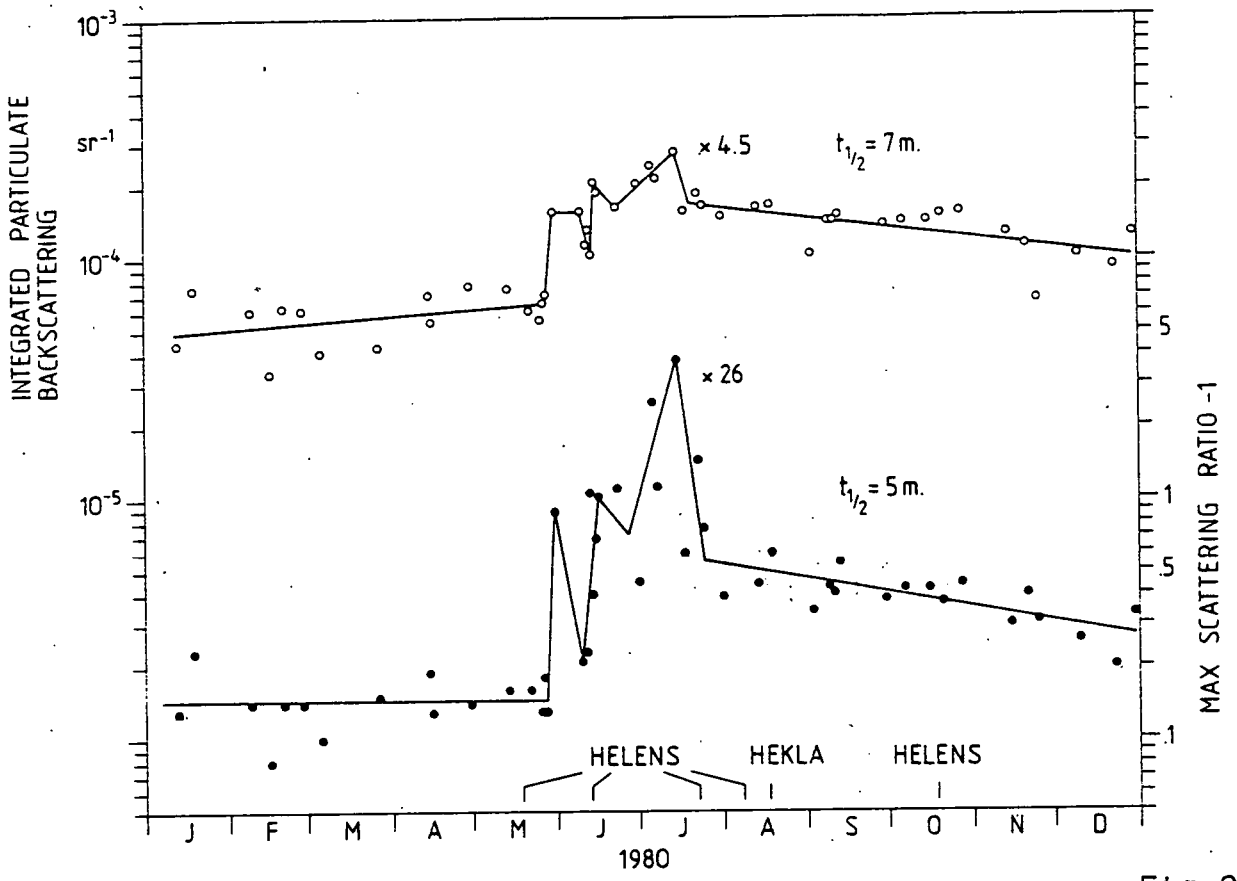
INTEGRATED PARTICULATE BACKSCATTERING
sr⁻¹
10⁻³
10⁻⁴
10⁻⁵
× 4.5
t1/2 = 7 m.
× 26
t1/2 = 5 m.
MAX SCATTERING RATIO -1
5
1
.5
.1
HELENS
HEKLA
HELENS
J F M A M J J A S O N D
1980

Fig.9

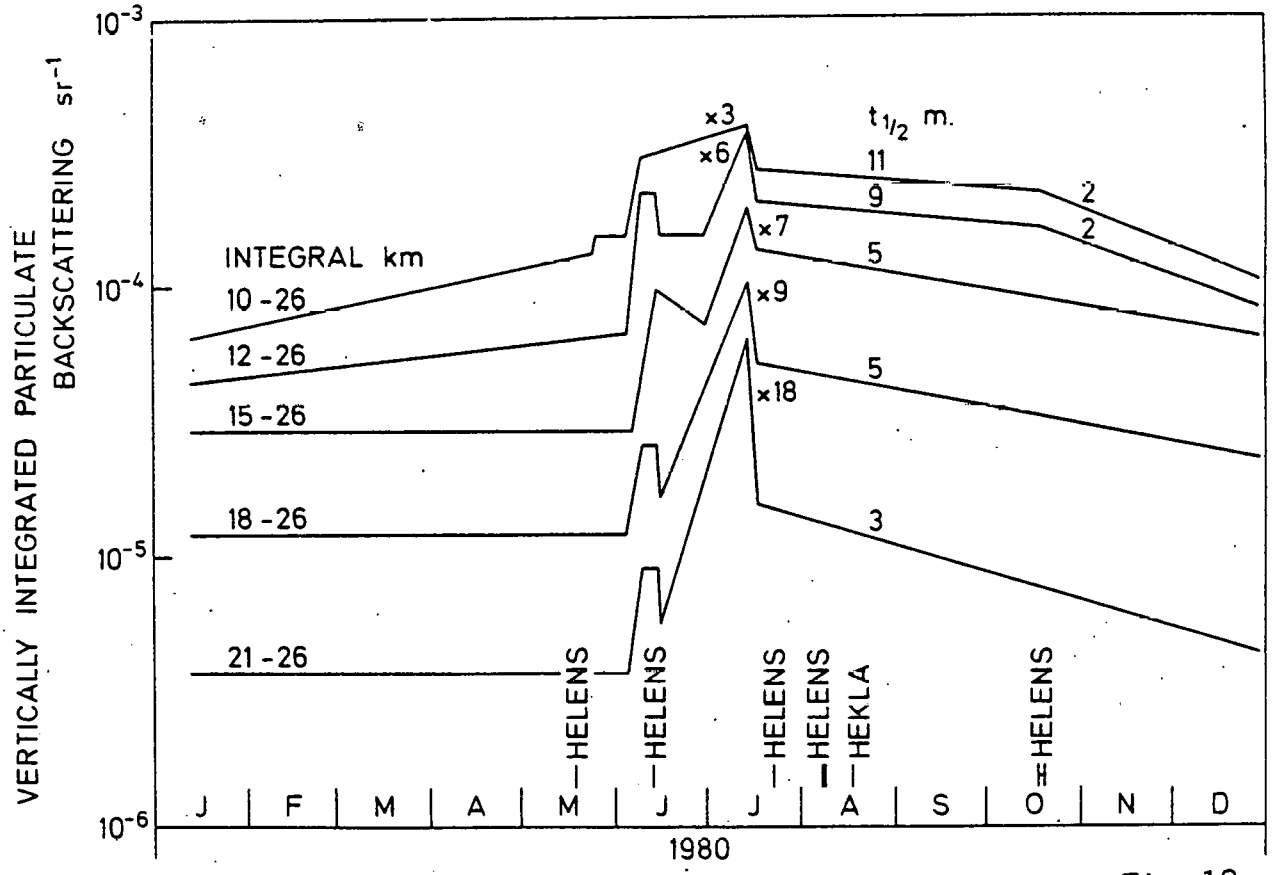
VERTICALLY INTEGRATED PARTICULATE BACKSCATTERING sr⁻¹
10⁻³
10⁻⁴
10⁻⁵
10⁻⁶
INTEGRAL km
10 - 26
12 - 26
15 - 26
18 - 26
21 - 26
×3
×6
×7
×9
×18
t1/2 m.
11
9
5
5
3
2
2
HELENS
HELENS
HELENS
HELENS
HEKLA
HELENS
J F M A M J J A S O N D
1980

Fig.10

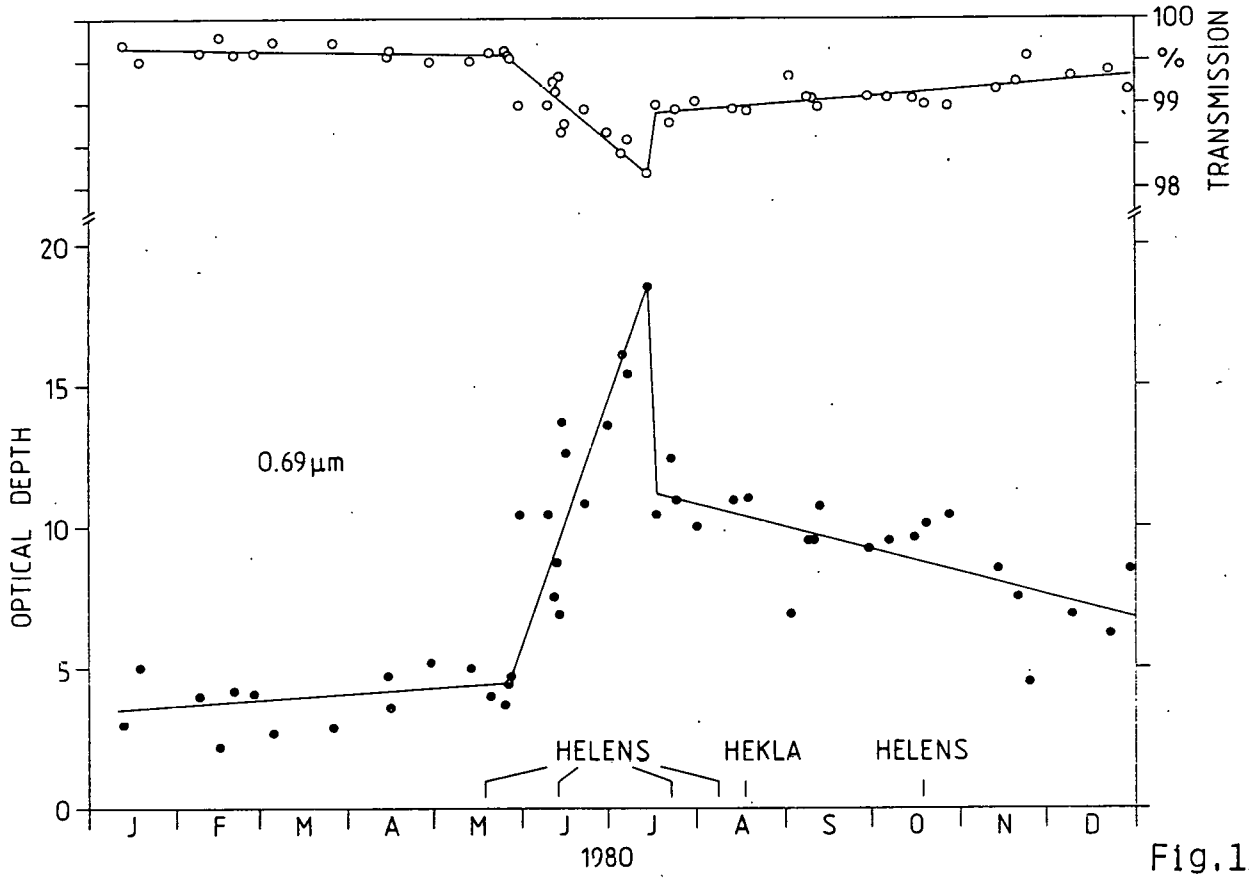
100
%
99
98
TRANSMISSION
20
15
10
5
0
OPTICAL DEPTH
0.69 µm
HELENS
HEKLA
HELENS
J
F
M
A
M
J
J
A
S
O
N
D
1980

Fig.11